Positron Emission Tomography and Radioimmunotargeting

Aspects of Quantification and Dosimetry

Mark Lubberink, Hans Lundqvist, Jan-Erik Westlin, Vladimir Tolmachev, Harald Schneider, Anna Lövqvist, Anders Sundin and Jörgen Carlsson

From the Sections of Biomedical Radiation Sciences (M. Lubberink, H. Lundqvist, V. Tolmachev, A. Lövqvist, J. Carlsson), Oncology (J.-E. Westlin), and Radiology (A. Sundin), Department of Oncology, Radiology and Clinical Immunology, Uppsala University, and Uppsala University PET Centre (H. Schneider), Uppsala, Sweden

Correspondence to: Dr Mark Lubberink, Uppsala University, Biomedical Radiation Sciences, Box 535, 751 21 Uppsala, Sweden. Tel: +46 18 471 38 29. Fax: +46 18 471 34 32. E-mail: Mark.Lubberink@bms.uu.se

Acta Oncologica Vol. 38, No. 3, pp. 343–349, 1999

Positron emission tomography (PET) is a medical imaging tool with high resolution and good quantitative properties, which makes it suitable for in vivo quantification of radioimmunotargeting agents. Most radionuclides used in radioimmunotherapy have positron-emitting analogues, which can be used for PET imaging, and this opens the possibility of performing dosimetry with PET. These isotopes, however, often emit gamma radiation and high-energy positrons in their decay, influencing the imaging properties of PET. Spatial resolution, reconstructed background and line source recovery for a number of non-pure positron emitters were investigated and compared with the imaging properties of ^{18}F. PET imaging properties did not degrade severely for these non-pure positron emitters, but caution has to be applied when doing quantitative measurements. To assess the possibility of conducting PET studies during therapy, by combining, for example, a small amount of ^{124}I with ^{131}I, the influence of the presence of large amounts of gamma radiation on PET count rate characteristics was studied. The results of these studies were related to the necessary amounts of radioactivity needed for treatment of post-operative remains of glioma. The results indicate that the count rate capabilities of 2D PET permit PET studies for dose evaluation during radioimmunotherapy.

Received 21 April 1998
Accepted 15 December 1998

To optimize radioimmunotherapy, information about specific uptake, kinetics, metabolic patterns and optimal administration in the individual patient is important. A major problem is the accurate determination of the absorbed dose in target organs, tumour tissue and critical organs (1). Positron emission tomography (PET) is an excellent tool for quantitative measurements of the in vivo distribution of substances labelled with positron-emitting isotopes. This distribution can be measured with a time resolution of less then 10 s, a spatial resolution of less than 1 cm, and the highest quantitative accuracy available for imaging of in vivo radioactivity distributions. Thus PET is suitable for measuring the uptake of radioimmunotargeting agents. However, all nuclides used in radioimmunotherapy emit electrons, and usually also gamma radiation, and these isotopes cannot be measured with PET. Generally, both spatially and quantitatively considerably less accurate techniques such as single photon emission tomography (SPECT) or planar scintigraphy (gamma camera) are used to measure the uptake of these nuclides. The labelling of targeting agents with positron-emitting nuclides frequently used in PET, such as ^{18}F, ^{11}C or ^{15}O, could be an option. However, the chemical and biological behaviour of these labelled targeting agents does not have to resemble the behaviour when labelled with therapeutic nuclides. Another drawback is the short half-lives of these nuclides, ranging from two minutes to two hours, much shorter than the physiologically relevant time for most targeting agents.

We developed methods for the production of positron-emitting nuclides with longer half-lives, such as ^{76}Br, ^{83}Sr, ^{72}As, ^{52}Fe, ^{110}In, and ^{86}Y (2). Several of these nuclides, as well as ^{124}I, also open the possibility of labelling targeting agents with positron-emitting analogues of the nuclides used in radioimmunotherapy (3). Here, the biological and chemical properties of the agent labelled with the positron-emitting nuclide and the therapeutic nuclide are identical. PET can then be used to study the in vivo distribution of

 ISSN 0284-186X

targeting agents accurately, to predict doses and to plan and evaluate therapy. So far, efforts in this direction have mainly been made for the analogues $^{124}I/^{131}I$ (4, 5), $^{86}Y/^{90}Y$ (6), and, in ongoing studies at our group, for $^{110}In/^{111}In$ (2). Several methods have been developed to perform to a certain extent patient-specific internal dosimetry, using, for example, the Mirdose program (7), or methods based on Monte Carlo simulations or dose-point kernels using SPECT or PET images for information on radioactivity uptake combined with co-registered CT or MRI images for anatomical information (8–11). We are currently investigating the possibility of predicting the ^{111}In-octreotide-therapy dose to a tumour using PET measurements with ^{110}In-octreotide and the Mirdose program (2).

A possible problem associated with the use of these nuclides in PET is the radiation emitted in their decay. The standard PET nuclides ^{18}F and ^{11}C are pure positron emitters, and the energy of the emitted positrons is relatively low, less than 1 MeV, which makes their range in biological tissue of the order of a few millimetres. The imaging properties of a radionuclide in PET are influenced by the energy of the emitted positrons and the amount of gamma radiation emitted in the decay of this nuclide. Another aspect influencing the accuracy of quantification is the density of the tissue. To investigate these effects we performed phantom studies with ^{76}Br (12), ^{83}Sr, ^{52}Fe, ^{52m}Mn, and for comparison also ^{18}F. These are not all nuclides that are relevant for radioimmunotherapy, but their decays have many similarities with, for example, ^{124}I, ^{110}In and ^{86}Y, concerning low positron abundance, high gamma abundance and the emission of gamma radiation in coincidence with positrons or other gamma radiation. Also, the half-life of ^{76}Br makes it suitable for labelling of, for example, monoclonal antibodies (12). Table 1 gives some decay characteristics of these nuclides. Similar studies have been carried out for ^{124}I (13), and these effects were theoretically predicted for a number of nuclides by Pagani et al. (14).

Table 1

Decay properties

Nuclide	% β^+	$E^+_{\beta,mean}$ (MeV)	$E^+_{\beta,max}$ (MeV)	% γ (>300 keV)
^{18}F	97	0.3	0.6	0
^{52}Fe	56	0.3	0.8	2
^{52m}Mn	97	1.2	2.6	100
^{76}Br	55	1.2	3.9	193
^{83}Sr	23	0.5	1.2	74
^{86}Y	32	0.7	3.1	315
^{110}In	62	1.0	2.3	98
^{124}I	27	0.8	2.2	96

Decay properties of relevant positron-emitting nuclides: positron abundance, mean and maximum positron energy and abundance of gamma radiation with energy >300 keV, the energy threshold of many PET systems.

Instead of using PET beforehand for dose planning, the possibility of using PET for dose evaluation during radioimmunotherapy, by adding a small amount of positron-emitting isotope to the therapeutic isotope, is also considered. Such an application could lie in the treatment of spread remains of glioma after operative removal of the bulk of the tumour by administration of a targeting agent labelled with ^{131}I directly into the remaining cavity, possibly combined with external irradiation (15). After administration, the iodine will be taken up into the surrounding tissue. The kinetics of the labelled targeting agent can be accurately followed in vivo using PET by adding a small amount of the positron-emitting isotope ^{124}I, so the delivered dose can be calculated accurately. We calculated the amounts of radioactivity typically needed for this application, and studied the effect of high concentrations of non-correlated gamma radiation on PET measurements of a positron-emitting nuclide.

MATERIAL AND METHODS

Tomograph

The experiments were carried out with a GEMS 4096 Plus tomograph (16) (Scanditronix AB, Uppsala, Sweden). This is a whole-body camera consisting of eight rings separated by non-removable septa, each of which contains 512 detectors, producing 15 image planes with a total axial field of view (FOV) of 10.5 cm. Transmission measurements with a rotating $^{68}Ge/^{68}Ga$ rod source were made for attenuation correction. All standard corrections for random coincidences, scattered radiation and dead time were used in the image reconstruction.

Radionuclide production

The nuclides ^{83}Sr and $^{52}Fe/^{52m}Mn$ were produced by the $^{85}Rb(p,3n)^{83}Sr$ and $^{nat}Ni(p,xn)^{52}Fe$ reactions at the Gustav Werner cyclotron (The Svedberg Laboratory, Uppsala, Sweden). Details concerning production routes and radionuclidic purity are given in (17) and (18), respectively. ^{76}Br was produced by the $^{76}Se(p,n)^{76}Br$ reaction according to method described in Tolmachev et al. (19). Details on the production of ^{110}In are given in (20). ^{113m}In was produced by the $^{114}Cd(p,2n)^{113m}In$ reaction using enriched ^{114}Cd metal (99.1% enrichment, Teknowledge UK Ltd., London) as a target. The target, with a thickness of 0.24 g/cm^2, was irradiated with protons with an energy of 16.4 MeV using a Scanditronix MC-17 cyclotron at Uppsala University PET Centre, and used for measurements immediately after bombardment.

Calibration

For each of the radionuclides used in these experiments a cross-calibration between the different detectors generally used in PET studies was made. These cross-calibration factors were related to an absolutely calibrated solid state

detector (EG&G Ortec Gamma-X high-purity germanium detector) to obtain absolute calibration factors.

Imaging properties

The spatial resolution and line source recovery in materials of different densities were measured using a phantom consisting of square sections made from polythene (1.0 g/cm^3), bonded foam (0.2 g/cm^3), and two kinds of wood (0.5 and 0.15 g/cm^3). A single catheter (Terumo Radifocus SP-catheter, Terumo Corporation, Tokyo, Japan) with an inner diameter of 0.5 mm was inserted through the middle of all phantom sections. By filling this catheter with a radioactive solution, we obtained a line source with the same radioactivity concentration in the middle of each phantom section. The dimensions of the different sections, $8 \times 8 \times 12$ cm^3 for the two higher density materials and $10 \times 10 \times 12$ cm^3 for the two lower density materials, were chosen so that practically all of the positrons emitted in the line source are stopped within the material. The phantom was placed in the centre of the field of view of the PET camera with each line source at 6–7 cm from the camera axis. After a transmission scan the catheter was filled with a radioactive solution of several tens of MBq, and emission data were collected for 10–20 min. The images were reconstructed using two different filters: a 1-mm ramp filter, for an optimal measure of the resolution, and a 4.2-mm Hanning filter, which is normally used in clinical studies at our centre. The standard corrections were applied. The spatial resolution in each material was determined as the average of the full widths at half maximum (FWHMs) of Gauss functions fitted to horizontal and vertical profiles through the point responses in all image planes. Line source recovery was calculated by determining the radioactivity in concentric regions of interest (ROIs) around each line source relative to the known line source radioactivity and plotting this as a function of the radius of the ROI.

To assess the accuracy of the applied corrections, a cylindrical polystyrene phantom (inner length 35 cm, inner diameter 19 cm) was used. The phantom contained a polythene rod (dimensions $19 \times 4 \times 4$ cm) positioned perpendicular to the cylinder axis. This rod provides a volume where no true unscattered coincidences of annihilation photons can be measured when the phantom is filled with a radioactive solution. The activity concentration measured in the rod, divided by the concentration measured in the solution, gives the scatter correction error (21), or in the case of non-pure positron emitters rather just the 'correction error'. The phantom was placed in the centre of the field of view of the PET camera with the rod parallel to the image planes. A transmission scan was taken of the phantom filled with water. Then a radioactive solution was diluted in the phantom and a 10–20-min emission scan was taken. The radioactivity concentration in the phantom was for all nuclides in the range of 10–25 kBq/ml. The images were reconstructed using a 4.2-mm Hanning filter and the standard scatter correction algorithm. The correction error was calculated by dividing the mean radioactivity concentration in a $1 \times 1 \times 15$-cm^3 volume of interest in two image planes in the centre of the cold rod by the mean radioactivity concentration in the radioactive solution.

Count rate performance with high gamma background.

A 370-MBq ^{68}Ge/^{68}Ga pin source (outer diameter c. 6 mm) was placed centrally on a head support, about 5 cm below the centre of the FOV of the whole-body camera. A small radioactive pellet (1 cm^2) containing 5.85 GBq of ^{113m}In ($t_{1/2} = 99.5$ min) was placed next to the pin, centrally in the axial FOV. This isotope was chosen because the only gamma radiation emitted in its decay, with an energy of 392 keV, is very similar to the main gamma radiation in the ^{131}I decay, which has an energy of 364 keV. The pellet also contained c. 1.5% radioactivity of a positron-emitting contamination consisting of other indium isotopes produced in the reaction described above. The emission data were collected for a total of 20 h, in 80 frames each 15 min long. The images were reconstructed using a 1-mm ramp filter, the standard random and scatter correction and without attenuation correction. Circular ROIs were drawn in the pin, the location of the pellet, and in the background around the centre of the FOV, in all of the 15 image planes.

Combination of ^{124}I and ^{131}I in PET during therapy

A condition for the use of ^{124}I with ^{131}I is that the radiation emitted by ^{131}I does not affect accurate PET imaging of ^{124}I. We calculated the radioactivity that has to be administered to deliver a dose of 60 Gy to the tissue surrounding a post-operative tumour cavity in the brain, assuming that the injected radioactivity is instantly taken up in the surrounding tissue. The self-dose can be calculated as the product of administered radioactivity, residence time and S-value according to the MIRD formalism. The self-dose S-value for a sphere of certain volume is approximately proportional to the volume of this sphere, and for a mainly beta-emitting isotope we can assume the same proportionality constant for the volume of a hollow sphere with certain thickness. The self-dose S-value for a hollow sphere with a certain inner radius R and thickness d is then:

$$S \approx 0.039 \cdot \left[\frac{4}{3} p((R+d)^3 - R^3) \right]^{-1} \quad [1]$$

with R and d in cm, and the constant 0.039 in [mGy·cm^3/MBq·s]. The proportionality constant was found by a linear least-squares fit of self-dose S-values versus sphere volumes, calculated in Mirdose. Using this approximation we determined the amount of ^{131}I-radioactivity that has to be administered to hollow spheres of different radii and thickness to obtain a self-dose of 60 Gy, and estimated the

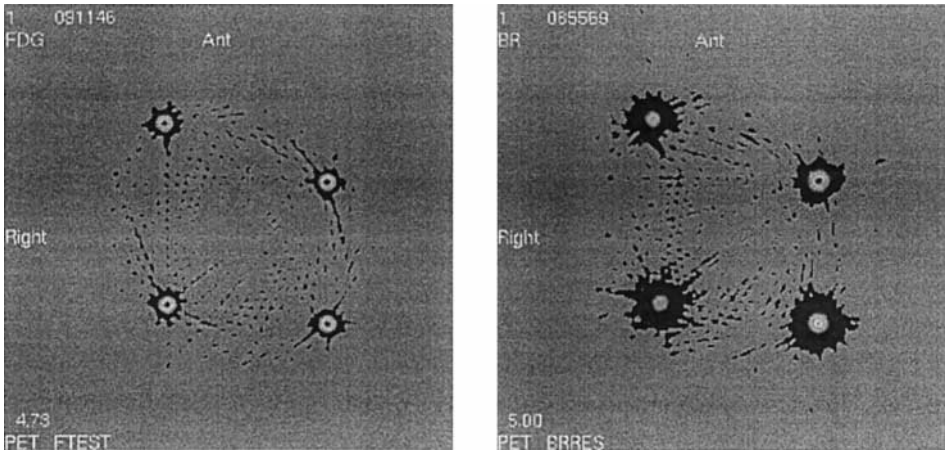

Fig. 1. Greyscale PET images of the resolution phantom for ^{18}F (left) and ^{76}Br (right). For clarity reasons the background colour has been modified from black to grey.

effect that this amount of ^{131}I activity would have on the accuracy of PET measurements.

RESULTS

Imaging properties

Fig. 1 shows a PET image of the phantom used in the resolution measurements with the catheter filled with a solution of ^{18}F and ^{76}Br. The transverse resolutions are given in Fig. 2 for all investigated nuclides in the event of a 1-mm ramp filter. The corresponding resolutions for a 4.2-mm Hanning filter were c. 1.5 mm worse. The standard errors given in the figure are the standard deviations between planes and directions. Fig. 3 shows the integrated point spread functions, or the recovery factor, in polythene (1.0 g/cm^3) and in bonded foam (0.2 g/cm^3). The correction errors are presented in Table 2. Some of these data were published earlier (2, 12).

Count rate performance with high gamma background

Fig. 4 shows the measured radioactivity in the pin-source, the pellet and the background in different slices. The activity measured in the pellet mainly originates from the positron contamination with a half-life of on average c. 60 min. The background activity in the image plane containing the ^{113m}In pellet increased with a factor 20 at a pellet activity of 5 GBq, but in planes closer to the edge of the axial FOV the background decreased during the first hours. In planes neighbouring the plane containing the pellet, but not in that plane itself, the radioactivity in the pin source was overestimated for almost 10 h.

Combination of ^{124}I and ^{131}I in PET during therapy

Fig. 5 gives the radioactivity that has to be administered to a hollow sphere, for a sphere with an inner radius of 1 cm and different thicknesses and residence times, to obtain a dose of 60 Gy.

DISCUSSION

The results show that PET spatial resolution degrades slightly and the applied corrections in the image reconstruction are less accurate for unconventional positron emitters emitting high-energy positrons and gamma radiation in their decay. This means that, in applications where the use of these nuclides is preferred because of the longer half-life or the analogy with therapeutic nuclides, quantitative measurements have to be done with more care than in the case of pure low-energy positron emitters such as ^{18}F.

Imaging properties

The transverse resolution of the used PET system degraded only slightly for the studied nuclides in comparison with ^{18}F. For the lower density scatter material, there was a small and expected degradation of the resolution for ^{18}F because of the higher positron range. This was also found for ^{83}Sr, but not for ^{76}Br, ^{52m}Mn and ^{52}Fe/^{52m}Mn. The basic reason for this difference in the relation between density and resolution lies in the shape of the positron energy distributions.

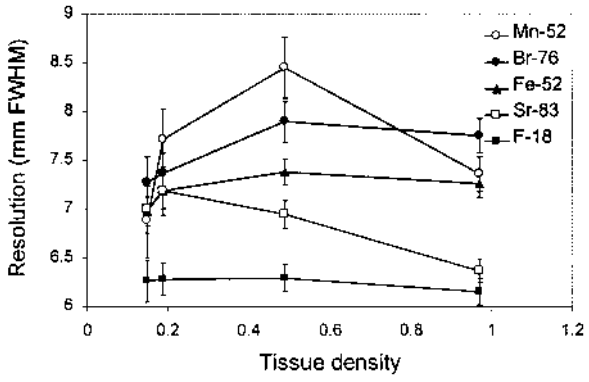

Fig. 2. Transverse resolution for different nuclides as a function of 'tissue' density.

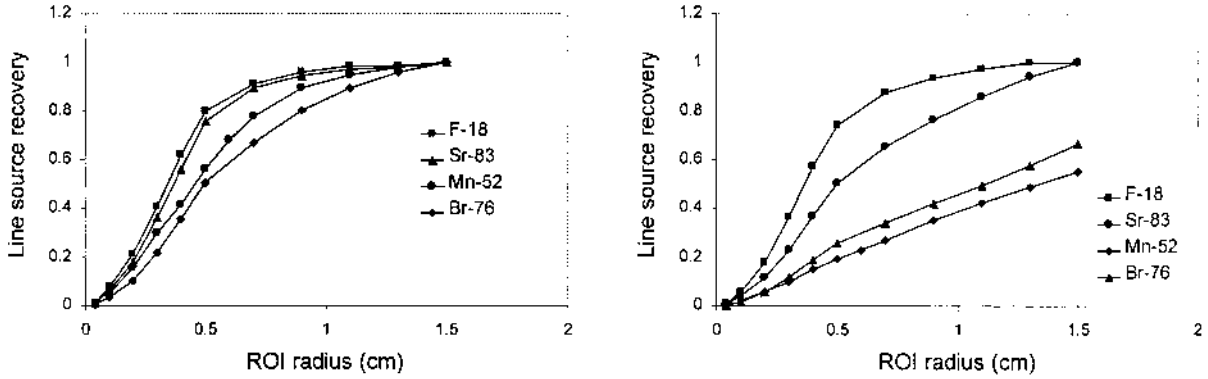

Fig. 3. Line source recovery for different radionuclides in polythene (1.0 g/cm^3, left) and bonded foam (0.2 g/cm^3, right) as a function of region of interest (ROI) radius. The line source recovery was determined as the total amount of radioactivity in a circular ROI around the line source, divided by the radioactivity in a 3-cm diameter ROI around the line source in polythene.

The amount of recovered radiation in a certain volume around the line source depends greatly on the density of the surrounding tissue. A larger area in the image is needed to recover the same relative amount of radiation for ^{76}Br, for example, than for ^{18}F. This means that quantitative measurements, mainly with ^{76}Br and ^{52m}Mn, have to be carried out with great care, especially in tissues of lower density such as the lungs or near sharp changes in density, for example around the heart.

The increase in reconstructed background is probably caused by the detection of essentially true coincidences of gamma radiation emitted in coincidence with the positrons or with other gamma radiation. This assumption is strengthened by the fact that the effect is largest for ^{76}Br, which emits most of this coincidence gamma radiation in its decay. In septa-less (3D) PET cameras, which have a higher acceptance for scattered radiation and random coincidences than 2D cameras, this effect will be larger. The increase in reconstructed background may affect quantification in another way: attenuation correction relatively increases this contribution in tissues with higher density, such as the bone. We are investigating this in ongoing studies.

Count rate performance

In Fig. 4 we can see that the PET camera saturates for the pellet radioactivity after c. 2 h, about 2.5 GBq. This saturation can be seen to a different extent in all the slices. The measured excess activity in the first hours also means that PET measurements begin to be less accurate at c. 1 GBq single photon activity. The increase in background caused by the single photons is small at low activity concentrations of a positron-emitting nuclide. For example, 50 MBq of a positron-emitting nuclide in the camera volume, or say 1000 Bq/ml together with 4 GBq (about the limit for saturation) of a therapeutic nuclide, would cause a background of 100 Bq/ml (from Fig. 4), i.e. 10%.

Combination of ^{124}I and ^{131}I in PET during therapy

^{131}I emits gamma radiation and electrons in its decay, with an abundance of 92% of gamma radiation with energy over 300 keV, the general PET threshold. ^{124}I emits 23.1% positrons and 96% gamma radiation, or 142% including the annihilation photons. This means that the total gamma abundance in a 10 : 1 ^{131}I-^{124}I preparation is 106%, and the positron abundance 2.3%. As seen above, our PET camera saturates for singles rates of $2.5 \cdot 10^9$ dps. Modern PET cameras, that can be operated with and without septa, saturate at a radioactivity concentration of c. 35 kBq/ml without septa (in 3D mode), or about eight times as much, 250 kBq/ml, in 2D mode (22), for a pure positron-emitting isotope diluted in a cylinder with a diameter of 20 cm and a length slightly greater than the axial FOV of the PET camera. The random coincidence rate of a radioactivity concentration of 250 kBq/ml pure positron emitter corresponds to 555 kBq/ml of the above described ^{131}I/^{124}I (10 : 1), based on the difference in gamma abundances. This corresponds to a total radioactivity of 2.5 GBq, neglecting coincidence gammas and higher random rates. In 3D PET the maximum amount of radioactivity is then $2.5/8 = 300$ MBq. As we can see in Fig. 5, for short residence times and

Table 2

Correction error

Nuclide	Correction error (%)
^{18}F	1
^{83}Sr	1
^{110}In	2
^{52}Fe/^{52m}Mn	2
^{76}Br	4

Correction error for a number of nuclides, determined as the measured radioactivity concentration in a cold insert divided by the radioactivity concentration in the surrounding radioactive solution, after correction for random and scattered coincidences and attenuation.

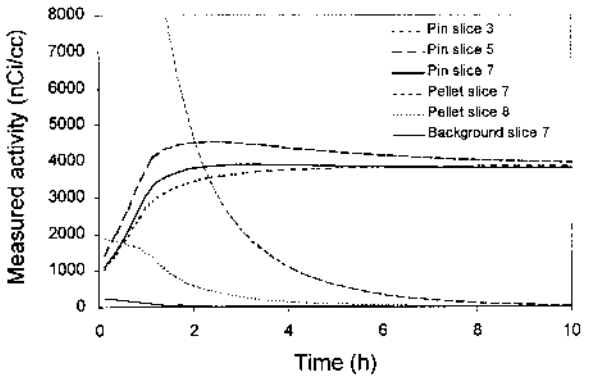

Fig. 4. Measured radioactivity in a ROI around the $^{68}Ga/^{68}Ge$ pin, in a ROI around the ^{113m}In pellet, and in the background of the image. The ^{113m}In pellet was placed in slice 7.

large tumour volumes the necessary amounts of radioactivity lead to inaccurate measurement of the ^{124}I radioactivity concentration in the PET camera, especially in 3D data acquisition. However, assuming not too large volumes and a residence time in the order of days, administration of a radioactivity below the maximum of 2.5 GBq results in a sufficient dose and the possibility of dose evaluation with 2D PET.

Using PET with positron-emitting isotopes from the same element as therapeutic nuclides offers a possibility for accurate dosimetry. A precondition is that there is a large enough overlap between the half-lives of the two isotopes. This, for example, is the case for $^{86}Y/^{90}Y$ and $^{124}I/^{131}I$. Dose calculation software using dose-point kernels or Monte-Carlo simulations, utilizing PET or SPECT measurements, has been developed, and less sophisticated methods using, for example, Mirdose also offer reasonable methods for internal dose calculations. For dose evaluation during radioimmunotherapy we would like to use a less expensive technique than PET, but we prefer also to be able to quantify the uptake correctly. A disadvantage of SPECT and gamma camera, compared with PET, is the relatively poor quantification. A possibility could be to 'calibrate' the gamma camera by first quantifying the radioactivity distribution in PET, and shortly afterwards making a gamma camera image to calculate a kind of correction factor and hence obtain quantitatively more accurate gamma camera information. The development of cheaper PET systems, such as rotating gamma camera systems capable of PET imaging (23, 24), could play an important role in further developments in this field.

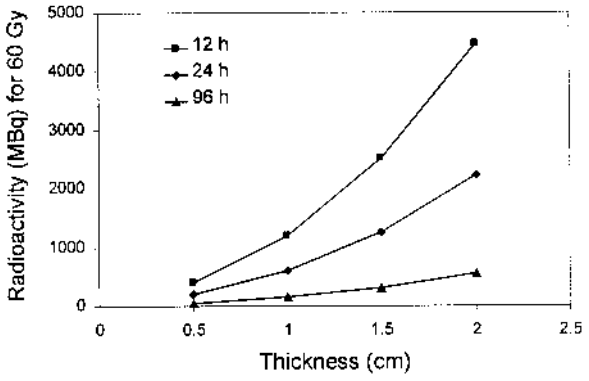

Fig. 5. Radioactivity that has to be administered to a hollow sphere to obtain a self-dose of 60 Gy, for a sphere with an inner diameter of 2 cm, as a function of sphere thickness.

ACKNOWLEDGEMENTS

The authors thank the staff at Uppsala University PET Centre and The Svedberg Laboratory for their technical assistance with PET measurements and nuclide production. Financial support was received from the Medical Faculty of Uppsala University, the Swedish Cancer Foundation and the Swedish Medical Research Council.

REFERENCES

1. Flower MA, McCready VR. Radionuclide therapy dose calculations: what accuracy can be achieved? Eur J Nucl Med 1997; 24: 1462–4.
2. Tolmachev V. Production and biomedical use of non-conventional positron emitters. Comprehensive Summaries of Uppsala Dissertations from the Faculty of Medicine. Uppsala: Acta Universitatis Upsaliensis, 1998.
3. Zweit J. Radionuclides and carrier molecules for therapy. Phys Med Biol 1996; 41: 1905–14.
4. Flower MA, Al-Saadi A, Harmer CL, McCready VR, Ott RJ. Dose-response study on thyrotoxic patients undergoing positron emission tomography and radioiodine therapy. Eur J Nucl Med 1994; 21: 531–6.
5. Larson SM, Pentlow KS, Volkow ND, et al. PET scanning of iodine-124-3F9 as an approach to tumour dosimetry during treatment planning for radioimmunotherapy in a child with neuroblastoma. J Nucl Med 1992; 33: 2020–3.
6. Herzog H, Rösch F, Stocklin G, Lueders C, Qaim SM, Feinendegen LE. Measurement of pharmacokinetics of yttrium-86 radiopharmaceuticals with PET and radiation dose calculation of analogous yttrium-90 radiotherapeutics. J Nucl Med 1993; 34: 2222–6.
7. Stabin MG. MIRDOSE: personal computer software for internal dose assessment in nuclear medicine. J Nucl Med 1996; 37: 538–46.
8. Furhang EE, Chui CS, Kolbert KS, Larson SM, Sgouros G. Implementation of a Monte Carlo dosimetry method for patient-specific internal emitter therapy. Med Phys 1997; 24: 1163–72.
9. Giap HB, Macey DJ, Bayouth JE, Boyer AL. Validation of a dose-point kernel convolution technique for internal dosimetry. Phys Med Biol 1995; 40: 365–81.
10. Kolbert KS, Sgouros G, Scott AM, et al. Implementation and evaluation of patient-specific three-dimensional internal dosimetry. J Nucl Med 1997; 38: 301–8.
11. Sgouros G, Chui CS, Pentlow KS, et al. Three-dimensional dosimetry for radioimmunotreatment planning. J Nucl Med 1993; 34: 1595–601.
12. Lövqvist A. On the use of ^{76}Br for radioimmuno PET. Experimental Studies. Comprehensive Summaries of Uppsala Dissertations from the Faculty of Medicine. Uppsala: Acta Universitatis Upsaliensis, 1996.

13. Pentlow KS, Graham MC, Lambrecht RM, Cheung NKV, Larson SM. Quantitative imaging of I-124 using positron emission tomography with applications to radioimmunodiagnosis and radioimmunotherapy. Med Phys 1991; 18: 357–66.
14. Pagani M, Stone-Elander S, Larsson SA. Alternative positron emission tomography with non-conventional positron emitters: effects of their physical properties on image quality and potential clinical applications. Eur J Nucl Med 1997; 24: 1301–27.
15. Blomquist E, Carlsson J. Strategy for planned radiotherapy of malignant gliomas: postoperative treatment with combinations of high dose proton irradiation and tumor seeking radionuclides. Int J Radiat Oncol Biol Phys 1992; 22: 259–63.
16. Rota Kops E, Herzog H, Schmid A, Holte S, Feinendegen LE. Performance characteristics of an eight-ring whole body PET scanner. J Comput Assist Tomogr 1990; 14: 437–45.
17. Tolmachev V, Lundqvist H. Production of ^{83}Sr for in vivo dosimetry. Neutron deficient nuclides for positron emission tomography. Moscow: Institute of Theoretical and Experimental Physics, 1995.
18. Tolmachev V, Lundqvist H, Einarsson L. Production of iron-52/manganese-52m generator. Neutron deficient nuclides for positron emission tomography. Moscow: Institute of Theoretical and Experimental Physics, 1994.
19. Tolmachev V, Lövqvist A, Einarsson L, Schultz J, Lundqvist H. Production of 76Br by a low-energy cyclotron. Appl Radiat Isot 1998; 49: 1537–40.
20. Lundqvist H, Tolmachev V, Bruskin A, Einarsson L, Malmborg P. Rapid separation of 110In from enriched Cd targets by thermal diffusion. Appl Radiat Isot 1995; 46: 859–64.
21. Karp JS, Daube-Witherspoon ME, Hoffman EJ, et al. Performance standards in positron emission tomography. J Nucl Med 1991; 12: 2342–50.
22. Wienhard K. PET state-of-the-art instrumentation. Physica Medica 1996; XII: 28–32.
23. Lundqvist H, Lubberink M, Tolmachev V. Positron emission tomography—nuclear physics applied in medicine. Eur J Physics 1998; 19: 537–52.
24. Links JM. Advances in nuclear medicine instrumentation: considerations in the design and selection of an imaging system. Eur J Nucl Med 1998; 25: 1453–66.